

Årgang LXXXIX, Nr. 3-4, september 2018

---

# BYGNINGSSTATISKE MEDDELELSER

*udgivet af*

DANSK SELSKAB FOR BYGNINGSSTATIK

Proceedings of the Danish Society for Structural Science and Engineering

---

Miguel Fernández Ruiz & Linh Cao Hoang  
The Elastic-Plastic Stress Field method for structural concrete design: a complementary perspective to the use of rigid-plastic design approaches.....45-73

KØBENHAVN 2021

*Eftertryk uden kildeangivelse ikke tilladt*  
*Copyright © 2021 "Dansk Selskab for Bygningsstatik", København*  
ISSN 1601-6548 (online)

Årgang LXXXIX, Nr. 3-4, september 2018

---

# BYGNINGSSTATISKE MEDDELELSER

*udgivet af*

DANSK SELSKAB FOR BYGNINGSSTATIK

Proceedings of the Danish Society for Structural Science and Engineering

---

Miguel Fernández Ruiz & Linh Cao Hoang  
The Elastic-Plastic Stress Field method for structural concrete design: a complementary perspective to the use of rigid-plastic design approaches.....45-73

KØBENHAVN 2021

Redaktionsudvalg

Lars German Hagsten (Redaktør)  
Rasmus Ingomar Petersen  
Finn Bach  
Sven Eilif Svensson  
Mogens Peter Nielsen  
Linh Cao Hoang  
Jakob Fisker

Artikler offentliggjort i Bygningsstatistiske Meddelelser har gennemgået review.  
Papers published in the Proceedings of the Danish Society for Structural Science  
and Engineering have been reviewed.

# **The Elastic-Plastic Stress Field method for structural concrete design: a complementary perspective to the use of rigid-plastic design approaches**

	Abstract	45
1	Introduction	46
2	Development of stress fields accounting for strain compatibility conditions	49
	2.1 The fundamentals of the Elastic-Plastic Stress Field method	50
	2.2 Generality of the approach	52
3	Implications of the strain state on the stress fields and associated structural responses	56
	3.1 Geometry and actions	57
	3.2 Design using rigid-plastic stress fields (Stringer Method)	58
	3.3 Discussion on the performance of the rigid-plastic solutions	61
	3.4 Behaviour of normally-reinforced elements	65
4	Conclusions	68
	Bibliography	71



# **The Elastic-Plastic Stress Field method for structural concrete design: a complementary perspective to the use of rigid-plastic design approaches**

Miguel Fernández Ruiz <sup>1</sup>

Linh Cao Hoang <sup>2</sup>

## **Abstract**

Limit analysis is a widely-used approach providing a comprehensive and consistent frame for design of structural concrete elements. This approach has traditionally been applied by engineers following a rigid-plastic formulation, which allows to perform hand-made analyses. Yet, the rigid-plastic approach shows a number of shortcomings, namely to consistently account for the strain and cracking state of the element in the response of the member. Within this frame, the Elastic-Plastic Stress Field (EPSF) method has been proposed as an alternative and complementary tool to rigid-plastic approaches. The EPSF shares the same background and provides stress fields consistent to those of rigid-plastic analyses. In addition, since they account for the material compatibility, the EPSF provide information on the displacement and strain field at failure and can be generated in an automated manner. The information of the strain field can further be used to account for several issues related to the compression softening behaviour due to transverse cracking or to determining the strains in the reinforcement and concrete at failure. In this paper, the fundamentals of the EPSF method are briefly introduced and discussed in relationship with rigid-plastic design approaches by means of a number of examples. On that basis, some design recommendations for application of these tools are stated.

---

<sup>1</sup> École Polytechnique Fédérale de Lausanne (EPFL), Switzerland

<sup>2</sup> Danmarks Tekniske Universitet (DTU), Denmark

## 1. Introduction

Design of structural concrete by means of equilibrium-based models can be traced back to the beginning of structural concrete analysis. Particularly, Ritter (1899) already presented at the end of the XIX<sup>th</sup> century the concept of truss models embedded in the concrete, where the tension elements were composed of reinforcement and the compression elements by the concrete. This pioneer work was later extended by Mörsh (1908) who consider also the potential spreading of the compression struts. These first attempts to provide designers with a consistent tool to design structural concrete elements on the basis of truss structures continued in an intensive manner thereafter in Germany. The works of Leonhardt and co-workers (Leonhardt and Walther, 1966) extended the original truss models (see Fig. 1a) to the resultants of elastic stress fields (determined on the basis of elastic solutions or photo-elasticity analyses). This opened the way to the strut-and-tie models, later formalized by Schlaich et al. (1982,1987), who gave a clear theoretical support to this technique (based on the theory of plasticity and energetic concepts).

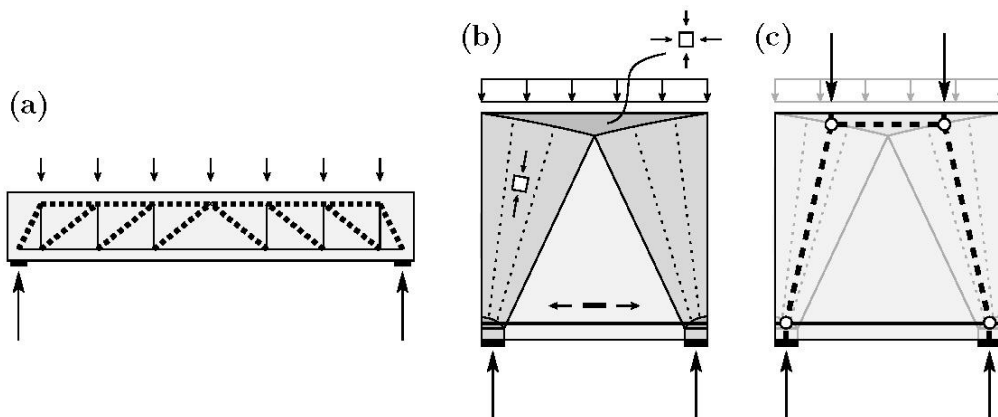


Figure 1 Equilibrium-based models for design: (a) truss model; (b) stress field; and (c) strut-and-tie model (resultant of forces of the previous stress field)

In parallel to these works on truss models and strut-and-tie models (developed initially in an intuitive manner), the theory of plasticity was formulated as well as its upper- and lower-bound theorems (Gvozdev 1938, Prager 1952). Following these works, Drucker (1961) proposed a series of exact solutions (satisfying both the lower- and upper-bound theorems of the theory of plasticity) for reinforced concrete beams. This approach allowed for the development of statically admissible and safe stress fields (in equilibrium with the acting loads and respecting the yield conditions of the materials, see Fig. 1b) by considering a rigid-plastic material response. The stress field approach started by Drucker was later extended, with significant contributions in Copenhagen (see for instance Nielsen and Hoang, 2011) and Zurich (see for instance Thürlimann et al. 1983 and Muttoni et al.

1997) and allowed for a consistent and comprehensive tool to design concrete structures.

As a natural convergence, both the strut-and-tie models and stress fields are used nowadays in an indistinct manner for the design of structural concrete elements. Both techniques are in fact complementary representations, one (stress fields, Fig. 1b) showing the stress state and required place for the compression fields and the other (strut-and-tie models, Fig. 1c) showing the location of the resultant of forces and being particularly suited for determining the force in the tension reinforcements.

Both techniques in their classical formulation rely eventually on the assumption of a rigid-plastic material behaviour. This makes the methods easy to use in practice but, on the other hand, creates a number of challenges and limitations. These include:

- Multiple solutions are possible for a given problem, requiring some level of experience for the user to decide on the most suitable one
- The solutions can be very safe and uneconomic or present problems at serviceability limit state (when the reinforcement is not arranged in the regions more prone to crack development)
- The effectiveness factor must be determined by calibration of the analytical solutions with tests for different cases (e.g. beam shear; torsion; bending; partially loaded areas, etc.). This is necessary as the effect transverse strains (and the associated crack widths) on the concrete strength cannot be determined (since rigid-plastic solutions do not provide information about the state of strain).
- Rigid-plastic design methods do not allow for specific checks on the required plastic deformation capacity. This aspect is relevant for structures where the stress fields considered for design needs significant redistributions to occur. Traditionally, this has been solved by requiring an enhanced plastic deformation capacity of the reinforcement (typically steel class B or C, see CEN 2004) or by limiting the size of the compression region in case of strain gradients (as for bending)

In order to overcome some of these challenges and limitations, further developments within the framework of rigid-plasticity have taken place in e.g. Denmark. This includes modification of the plastic solutions for members with and without shear reinforcement to account for effects of cracking (see for instance Nielsen and Hoang 2011, Jensen 2011, Fisker and Hagsten 2016); formulation of effectiveness factors which account for effects of transverse bursting stresses (see e.g. Zhang 1997 and Hoang et al. 2012); and most recently development of finite ele-

ment limit analysis, which employs numerical optimization to in all cases to obtain the exact solution (see e.g. Larsen 2010 and Herfelt 2017).

The above mentioned limitations have also motivated works performed in Switzerland, where numerical techniques for developing simple stress fields accounting for compatibility conditions have been developed (Fernández Ruiz and Muttoni 2007). The simplest approach that can be followed in this respect is probably the implementation of Elastic-Plastic calculations. Results obtained in this way may be called Elastic-Plastic Stress Fields (EPSF). In the simplest form, the EPSF considers a linear-elastic material behaviour, which is followed by a plastic behaviour once the yield condition is reached. For the concrete, consistently with experimental evidences, the level of the plastic plateau in compression is influenced by the state of strains of the element, allowing to account for the influence of transverse cracking on the material response (Vecchio and Collins 1986). In tension, no strength is considered. This latter aspect is instrumental to ensure consistency with rigid-plastic solutions and allows the approach to be robust from a numerical point of view (extensive comparisons to test results can be found in Muttoni et al. 2016). In fact, the EPSF can be seen as a tool in-between hand-made rigid-plastic analyses and complex (full non-linear) stress fields.

With respect to rigid-plastic solutions obtained by hand calculations, the EPSF offers also some valuable advantages:

- Since the analysis accounts for compatibility conditions, one solution is obtained for a given structure and set of actions. This allows obtaining suitable stress fields in an automated manner.
- The failure load of the element (when the applied loads cannot be further increased) corresponds to the exact solution according to limit analysis. This is justified as the stress field is in equilibrium with the actions and fulfils the yield conditions of the material (thus being a lower-bound of the failure load, see Fig. 2a-c) but its displacement field also corresponds to that of a geometrically possible mechanism respecting the compatibility conditions of the materials and the boundary conditions of the structure (thus being an upper-bound of the failure load, see Fig. 2d)
- Explicit checks on the level of strain of the concrete and reinforcement can be performed. For the latter, a suitable bond model is to be considered allowing also for estimating crack widths (Mata Falcón, 2015). This possibility is particularly convenient for instance to verify the deformation capacity of the reinforcement in case of significant plastic redistributions or low reinforcement ratios.

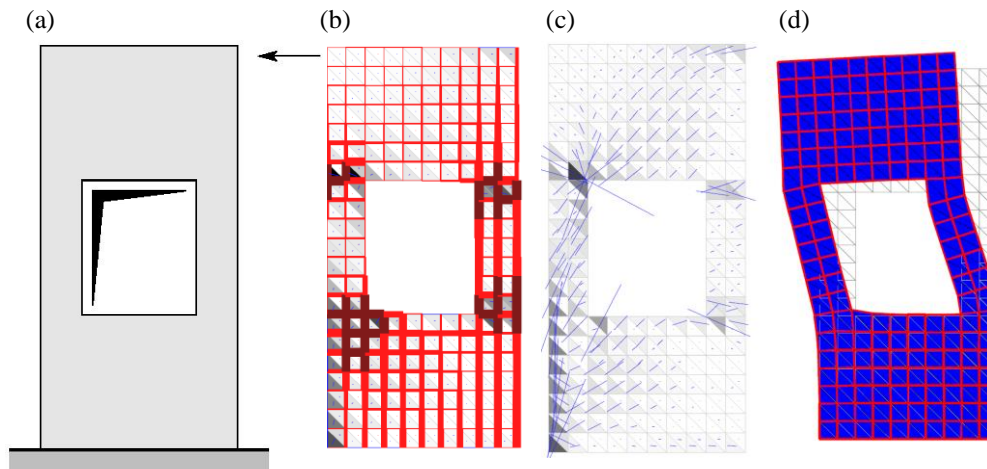


Figure 2: Elastic-Plastic Stress Field analysis: (a) structural model; (b) reinforcement stresses (red for tension, blue for compression, brown for yielded reinforcement) at failure; (c) concrete stress field (principal directions in blue, black meaning concrete crushing) at failure; and (d) associated displacement field at failure

In this paper, a brief summary of the principles for establishing EPSF will be commented, highlighting its advantages with respect to conventional (rigid-plastic) stress fields. An example of application will further be discussed, concerning the design of a load-deviation wall. This element, commonly used in practice, can be designed in different manners (with stiff or soft stringers). Although its response by assuming a rigid-plastic design model shall be identical, it will be shown that the actual response based on EPSF may significantly vary depending on the stringer stiffness and state of deformations and not all design possibilities exhibit the same level of performance. On that basis, a number of practical recommendations will be stated.

## 2. Development of stress fields accounting for strain compatibility conditions

The EPSF can be seen as a simple approach to produce in an automated manner admissible and safe stress fields accounting for compatibility conditions. This is performed by considering an elastic-plastic response of the materials and requires to consider, in addition to the plastic strength used in rigid-plastic analyses, the modulus of elasticity of the concrete and of the reinforcement. The limited number of material parameters makes the results of EPSF relatively easy to understand by the engineers. Furthermore, information on the displacement field and strain field of the structure is obtained, which can be used for a refined estimate of the effectiveness factors as it will later be discussed. This tool has been validated with test results on different structural elements and failure modes showing consistent and accurate agreement (systematic comparisons to test results can be found in Muttoni et al. 2016).

### 2.1 The fundamentals of the Elastic-Plastic Stress Field Method

To generate EPSF, the procedure generally followed is based on a finite element implementation (see for instance Fig. 3a) and consists of the following steps:

- The structure is defined with its properties, actions and boundary conditions. Materials are characterized by the modulus of elasticity and plastic strength. For the steel, the plastic strength corresponds directly to the yield strength of the material ( $f_y$ , Fig. 3b). For the concrete, the equivalent plastic strength ( $f_{cp}$ ) is obtained from the uniaxial compressive strength of concrete ( $f_c$ ), but reducing it by a brittleness factor ( $\eta_{fc}$ ) to account for the material compression softening response (Fig. 3c):

$$f_{cp} = f_c \cdot \eta_{fc} \quad (1)$$

, where factor  $\eta_{fc}$  is calculated according to the following expression (Muttoni 1989, fib 2013) accounting for the enhanced brittleness of high-strength concrete:

$$\eta_{fc} = \left( \frac{30 [\text{MPa}]}{f_c} \right)^{1/3} \leq 1.0 \quad (2)$$

It should be noted that the descending variation of  $\eta_{fc}$  with respect to  $f_c$  is very similar to the variation of the effectiveness factors,  $\nu$ , usually adopted for rigid-plastic analyses (CEN 2004).

- A displacement field is assumed. On that basis, the strain field is calculated for each element (Fig. 3d, Fernández Ruiz and Muttoni 2007)
- For the steel, the stress and associated nodal forces for each element are determined by using a stress-strain diagram (Fig. 3b, normally assumed as elastic-plastic, but also strain hardening can be introduced)
- For the concrete, the principal strain directions are calculated for each element. The associated stress field is determined by assuming that the principal stress directions are parallel to the principal strain directions (Fig. 3d, see also Fernández Ruiz and Muttoni 2007). For each principal direction, an elastic-plastic behaviour of concrete is assumed in compression with no tensile strength (Fig. 3c). This enables determining the principal stresses on the basis of the acting strain in the same direction. Yet, with respect to the plastic plateau in each principal direction, its strength is considered to be influenced by the state of transverse strains (principal strains in the other principal direction). When concrete is in biaxial compression, the

strength is maintained equal to the uniaxial material strength (no consideration of Kupfer’s biaxial increase of strength, Fig. 3e). When concrete is transversally in tension, cracking may occur reducing the compressive strength of concrete. This fact is considered by means of a strain reduction factor  $\eta_\varepsilon$  (Fig. 3f), which reduces the value of the effective plastic plateau of concrete:

$$\sigma_c \leq f_c \cdot \eta_{f_c} \cdot \eta_\varepsilon \tag{3}$$

The value of the coefficient  $\eta_\varepsilon$  can be calculated for instance according to Vecchio and Collins (1986) as:

$$\eta_\varepsilon = \frac{1}{0.8 + 170\varepsilon_1} \leq 1.0 \tag{4}$$

It can be noted that this reduction is performed locally, depending on the strain state of each element and varies with the level of load and applied actions.

- The equilibrium of the nodal forces is checked at each node for the assumed displacement field (on the basis of its associated stress fields and of the external actions). In case the equilibrium conditions are not satisfied within the accuracy required, a new displacement field is analysed (these iterations can be performed by using a Newton-Raphson numerical procedure, see Fernández Ruiz and Muttoni, 2007)

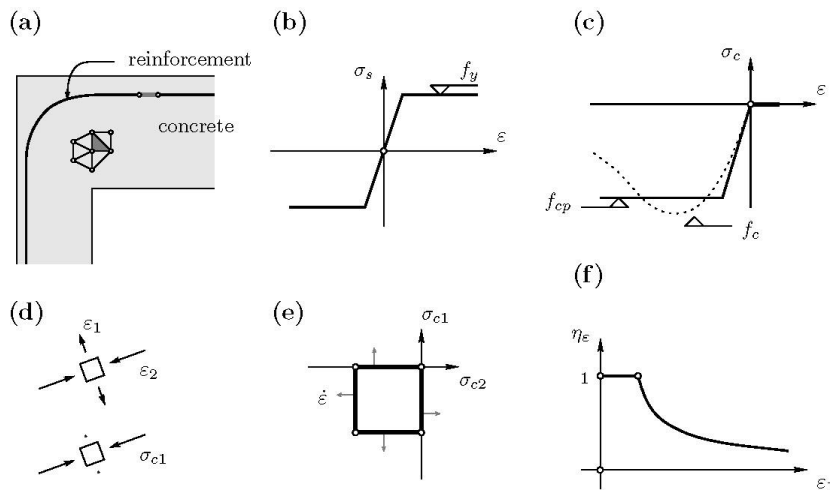


Figure 3: The Elastic-Plastic Stress Field Method: (a) model and mesh; (b) reinforcement material response; (c) concrete uniaxial material response; (d) concrete principal strain and stress directions; (e) (plane stress) Mohr-Coulomb plasticity condition with tension cut-off; and (f) concrete softening factor with transverse strains

The EPSF method has the advantage that, other than an admissible and safe stress field (in equilibrium node-by-node with the actions and where the yield conditions are respected at all elements), it ensures the compatibility of deformations, thus providing valuable information on the displacements, strains and crack widths (Mata Falc3n, 2015). This allows for realistic estimates of the strength reduction factor of concrete accounting for cracking ( $\eta_\epsilon$ ). In fact, it can be noted that the classical estimates of the concrete efficiency factor  $\nu$  (normally assumed constant for the member) can be replaced locally (finite element by finite element) by the multiplication of the brittleness and strain reduction factors:

$$\nu = \eta_{fc} \cdot \eta_\epsilon \quad (5)$$

Another advantage of the EPSF is that at failure (maximum load), the number and location of plasticized zones is in fact such that the displacement field corresponds to that of a geometrically possible mechanism (see Fig. 2d). As a consequence, the EPSF can be used to obtain exact solutions (being at the same time a lower- and an upper-limit of the failure load) according to the theory of plasticity.

The fact that exact solutions can be obtained by using the EPSF has implications both for design and for assessment of existing structures (an extended discussion can be found in Muttoni et al. 2015). For design, this is mostly relevant when an optimization of the member is needed (typically interesting in complex or repetitive (precast) members). It is however not so necessary for design of simple members, where rigid-plastic solutions can be safely used and often with less time consumption. The possibility to produce exact solutions is however very relevant for the assessment of existing structures. In this case, a refined and tailored analysis of the structure can avoid expensive strengthening or minimize it, implying significant cost savings.

## 2.2 *Generality of the approach*

An example showing the generality and consistency of this tool is presented in this section with reference to the shear walls investigated by Cardenas et al. 1980 (extensive and systematic validations of the tool with databases can be found in Muttoni et al. 2016). The investigated shear walls were tested under monotonic loading by applying a horizontal force until failure (see Fig. 4). Within the experimental programme of Cardenas, various reinforcement layouts were investigated (Fig. 5) yielding to different failure modes and resistances (Cardenas et al. 1980).

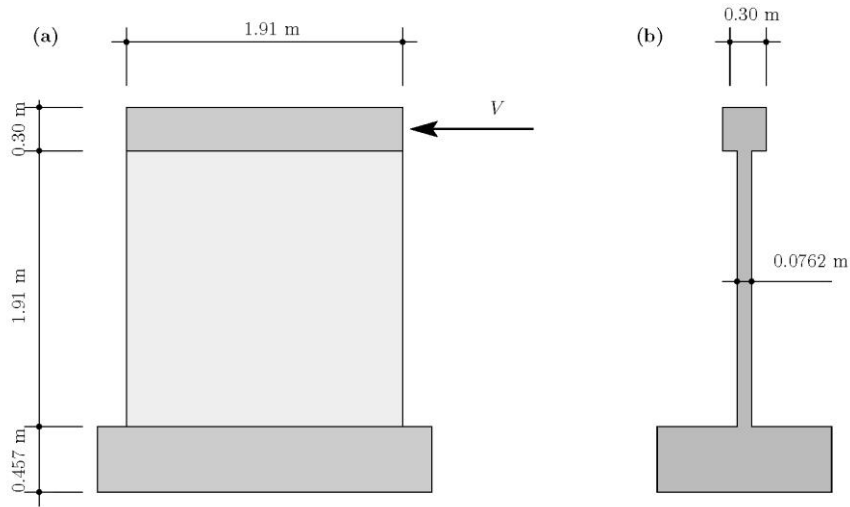
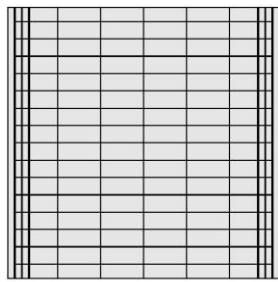
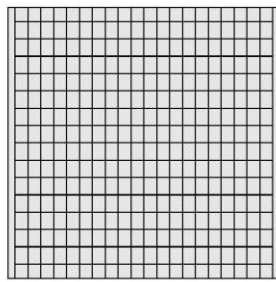


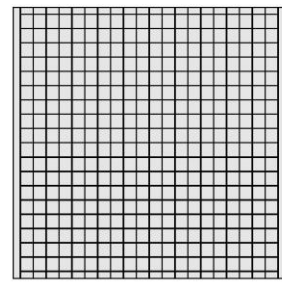
Figure 4: Geometry of the specimens tested by Cardenas et al. (1980): (a) view; and (b) cross-section



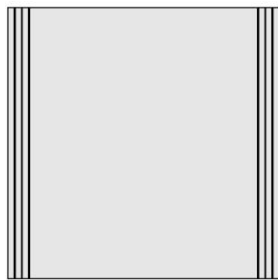
**SW7**,  $V_R = 539$  kN  
 $\rho_{w,h} = 0.27\%$  ( $f_y = 413$  MPa)  
 $\rho_{w,v} = 2.3\%$  ( $\frac{1}{3}$  per stringer,  $f_y = 448$  MPa)  
 $f_c = 43.0$  MPa



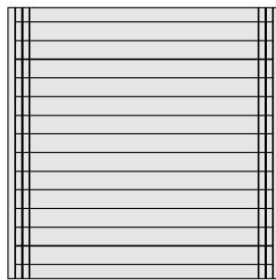
**SW8**,  $V_R = 575$  kN  
 $\rho_{w,h} = 0.27\%$  ( $f_y = 465$  MPa)  
 $\rho_{w,v} = 3\%$  ( $f_y = 448$  MPa)  
 $f_c = 42.4$  MPa



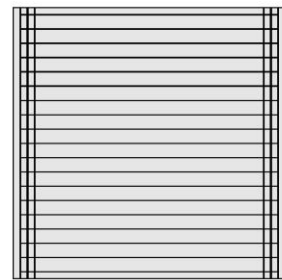
**SW9**,  $V_R = 685$  kN  
 $\rho_{w,h} = 1.00\%$  ( $f_y = 413$  MPa)  
 $\rho_{w,v} = 3\%$  ( $f_y = 448$  MPa)  
 $f_c = 43.0$  MPa



**SW10**,  $V_R = 306$  kN  
 $\rho_{w,h} = -$   
 $\rho_{w,v} = 1.65\%$  ( $\frac{1}{2}$  per stringer,  $f_y = 448$  MPa)  
 $f_c = 40.3$  MPa



**SW11**,  $V_R = 616$  kN  
 $\rho_{w,h} = 0.75\%$  ( $f_y = 448$  MPa)  
 $\rho_{w,v} = 2.3\%$  ( $\frac{1}{2}$  per stringer,  $f_y = 448$  MPa)  
 $f_c = 38.2$  MPa



**SW12**,  $V_R = 661$  kN  
 $\rho_{w,h} = 1.00\%$  ( $f_y = 448$  MPa)  
 $\rho_{w,v} = 2.3\%$  ( $\frac{1}{2}$  per stringer,  $f_y = 448$  MPa)  
 $f_c = 38.4$  MPa

Figure 5: Reinforcement layout of the shear walls tested by Cardenas et al. (1980)

The experimental results by Cardenas show that when the failure load is normalized by the thickness and lever arm of the member ( $z$  calculated as 1.62 m), the experimental results show increasing resistance with increasing amount of transverse (horizontal) reinforcement, see Fig. 6, with maximum values of the shear stress of about 5.5 MPa (specimen SW9) corresponding to flexural failures. It can be noted that even when no horizontal reinforcement was provided (specimen SW10), the member still showed a significant capacity to resist shear forces due to the direct load strutting that can develop for such small slenderness (average shear stress at failure equal to 2.5 MPa in this case). These experimental results are compared (also in Fig. 6) to the numerical predictions obtained with EPSF. The comparison shows a satisfactory and consistent agreement for the different cases investigated (average of measured-to-calculated strength equal to 0.98 with 5.0% of Coefficient of Variation).

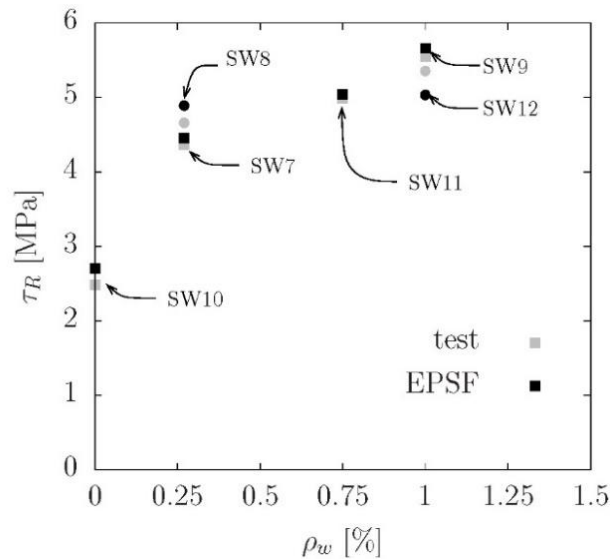


Figure 6: Comparison of test results and EPSF analysis

Some additional results are also presented in Fig. 7 for three representative cases (SW10 without horizontal reinforcement in Fig. 7a, SW7 with a moderate amount of horizontal reinforcement in Fig. 7b and SW9 with a high amount of horizontal reinforcement in Fig. 7c). The results are presented in terms of the steel and concrete stresses (top and bottom figure respectively for each specimen). The stresses in the reinforcement show that as the horizontal reinforcement ratio increases, the stress field modifies from a direct strut action (tension force in the flexural (vertical) reinforcement constant) to a beam action (with varying force in the tension flexural (vertical) reinforcement). This result is also consistently observed in the compression field of the member. It is interesting also to note that EPSF allow investigating cases where failure occurs prior to any steel yielding (specimen SW10) or that occur after yielding of the reinforcement (SW7 and SW9).

An additional result is also presented in Figure 8 for the load-deflection response of specimen SW9 (the only complete curve reported Cardenas et al. 1980). The results show that for low levels of load, the stiffness is underestimated by the EPSF as the tensile strength of concrete is not considered in the analysis. For high levels of load, on the other hand, the total stiffness can be overestimated as no degradation on the concrete stiffness is considered. This behaviour is consistent to other analyses performed with this technique (Fernández Ruiz and Muttoni 2007) and shows that reasonable estimates of the deflection and strains can be obtained even for the simple hypotheses adopted by the method.

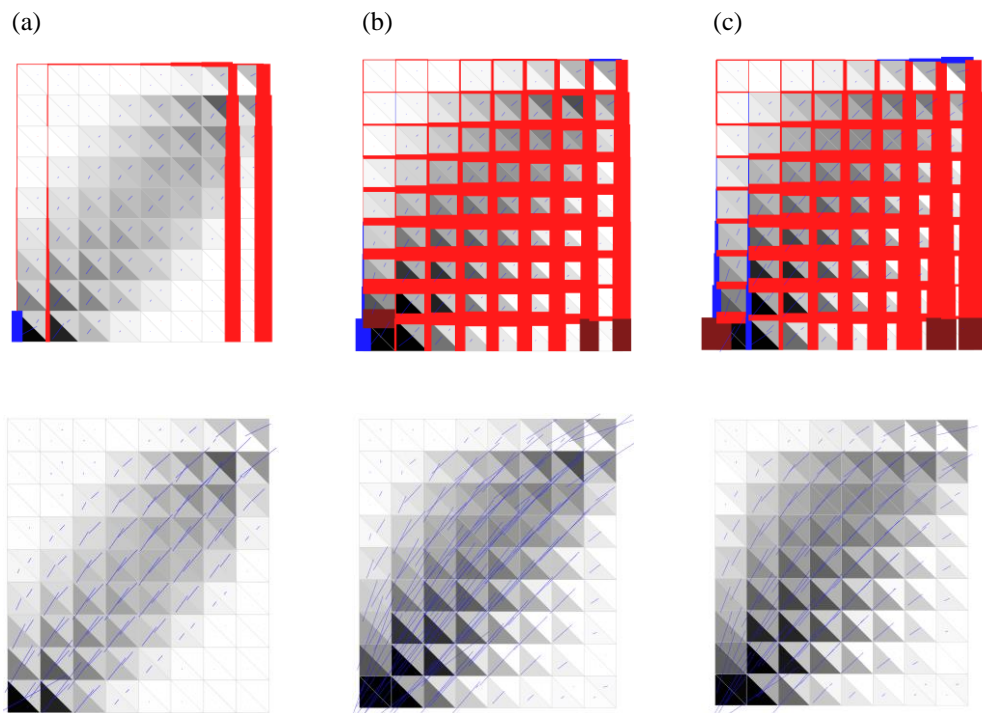


Figure 7: EPSF results for specimens: (a) SW10; (b) SW7; and (c) SW9 (top figures refer to the forces in the reinforcement: red for tension, blue for compression and brown for reinforcement yielding; bottom figures refer to the principal stress directions of concrete and calculated utilization ratio ( $\sigma_c / (f_{cp} \cdot \eta_\epsilon)$  where black means concrete crushing))

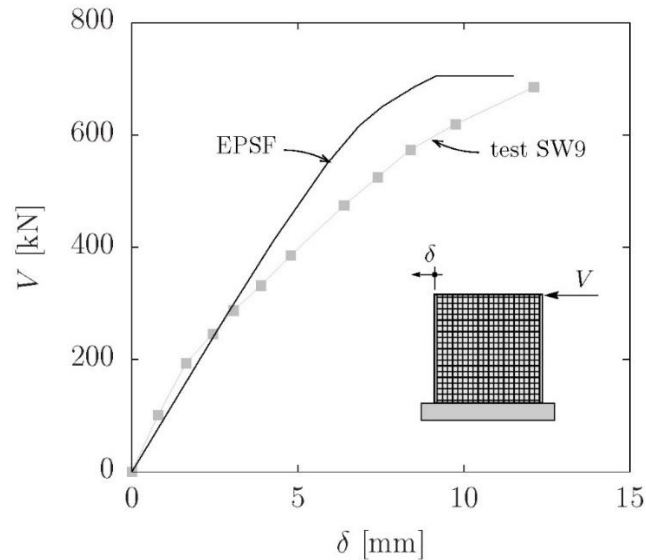


Figure 8: Measured and calculated load-deflection response for specimen SW9

### 3. Implications of the strain state on the stress fields and associated structural responses

An important aspect when designing concrete structures with rigid-plastic stress fields is to ensure the consistency between the resulting stress field and the actual structure. This holds true not only for the geometry, reinforcement and potential openings, but also to the manner in which the structural elements are defined.

For instance, an issue generally encountered refers to the stiffness to be provided to the stringers or diaphragms of a stress field model. This aspect has been covered in design approaches by rules of good practice, which can be based on minimum stiffness requirements or minimum strength requirements. For instance, in Denmark it is normally assumed that in a compression stringer, not more than 50% of the stringer force shall be carried by the reinforcement. This sets a (minimum) limit on the size of the concrete cross-section and, eventually, influences the manner in which the stringer transfers the load into the neighbouring elements. In other design traditions whose design guidelines are also extensively based on limit analysis and stress fields, such conditions are not provided and the amount of the load carried by the concrete and by the steel can be freely selected by the designer (refer for instance to the Swiss Code for structural Concrete SIA 262:2013). In this section, this question on the necessity and suitable stiffness to be provided to the stringers will be investigated on the basis of a case study on a load-deviation wall. This example will further allow discussing on the influence of the strain state on the overall response and on the pertinence of rigid-plastic design methods.

### 3.1 Geometry and actions

The investigated case corresponds to the deviation wall shown in Figure 9. The deviation wall is assumed to be cast in normal strength concrete C30/37 ( $f_{ck} = 30$  MPa) and allows to transfer the load between two non-aligned columns of two different storeys (distance between axis of columns equal to 3.0 m). The equilibrium of moments is eventually ensured by the slabs, which are assumed to transfer in a rigid manner the resulting horizontal forces to the cores of the building.

The wall is assumed to have a thickness of 250 mm and the columns to carry a load  $N_d = 3700$  kN (self-weight and actions from the slab are neglected). This load is transmitted by precast columns in high-strength concrete with a cross-section of  $250 \times 250$  mm<sup>2</sup> (average pressure at the support plate of the column equal to 59.2 MPa). The slabs also have a thickness of 250 mm and the distance between axis of the storeys is equal to 3 m ( $H_d = 3700$  kN thus by equilibrium). It can be noted that this geometry corresponds to a typical case where saving of ground floor by making use of small columns is governing for architectural reasons.

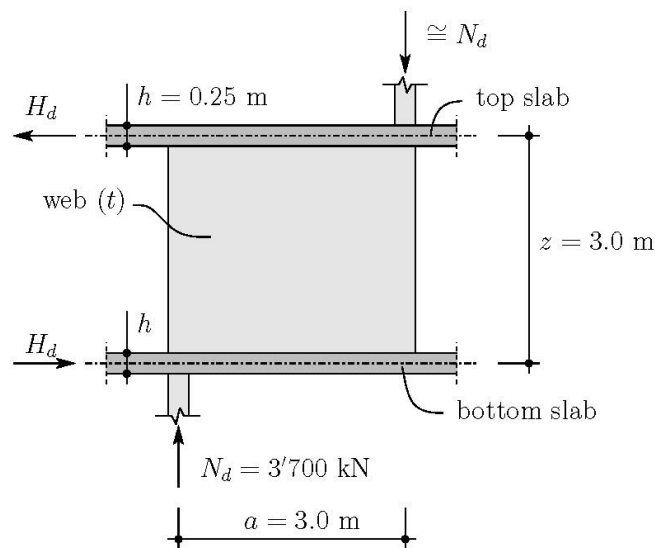


Figure 9: Geometry of the investigated load-deviation wall

### 3.2 Design using rigid-plastic stress fields (Stringer Method)

#### 3.2.1 Design of the web thickness

For design of the member, several choices shall be made, namely the thickness of the member and the reinforcement arrangement. With respect to the minimum thickness of the wall, it is controlled by the crushing conditions of the concrete struts. Since the pressure at the support plate is higher than the concrete strength

of the wall, it is proposed in this case a simple stress field with a constant compression field utilizing all available concrete within the wall (in accordance to what in Denmark is known under the term Stringer Method). Such stress field is shown in Fig. 10 together with its corresponding strut-and-tie model (refinements of the stress field by considering partial strutting of the load will be discussed later).

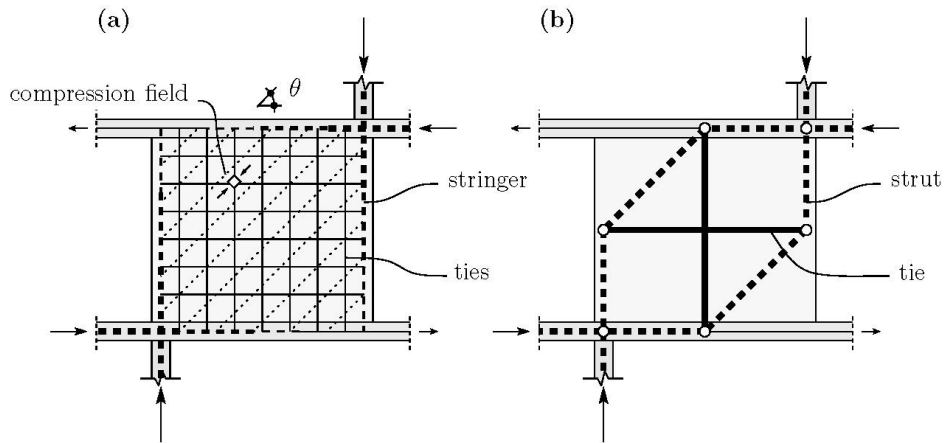


Figure 10: Rigid-plastic design of the load-deviation wall: (a) stress field (Stringer Method); and (b) corresponding strut-and-tie model

The design crushing condition of the compression field can be formulated in a simple manner as:

$$\tau_{Rd,max} = \frac{1}{2} \nu \frac{f_{ck}}{\gamma_c} \quad (6)$$

, which corresponds to an angle  $\theta$  of the concrete struts (refer to Fig. 10) equal to  $45^\circ$  to maximize the strength of the member. In this case  $\nu = 0.7 - f_{ck}/200 = 0.55$  according to the Danish design practice. It is interesting to note that the same value is obtained by use of Eq. (5) since  $\eta_{fc} = 1.0$  and  $\eta_\varepsilon$  may be taken as 0.55 according to MC2010 (fib, 2013). With  $\gamma_c = 1.5$ , the shear stress corresponding to concrete crushing is thus  $\tau_{Rd,max} = 5.5$  MPa and the acting shear stress results to:

$$\tau_{Ed} = \frac{N_d}{t \cdot z} \quad (7)$$

Since  $\tau_{Ed} \leq t \tau_{Rd,max}$ , the required width of the wall results in  $t \geq 224$  mm. In the following, a value of 250 mm will be adopted. For this wall thickness, the acting shear stress becomes finally  $\tau_{Ed} = 4.93$  MPa ( $< 5.5$  MPa).

### 3.2.2 Design of the reinforcement

For design of the mesh reinforcement in the wall, the reinforcement formulas for plane stress problems are used. For the case of pure shear action, the necessary reinforcement ratios in the  $x$ - and  $y$ -directions may be determined as:

$$\begin{aligned}\rho_x &= \frac{\tau_{Ed}}{f_{yd}} \cot \theta \\ \rho_y &= \frac{\tau_{Ed}}{f_{yd}} \frac{1}{\cot \theta}\end{aligned}\quad (8)$$

where  $f_{yd} = 435$  MPa (Class B500 steel with  $f_{yk} = 500$  MPa and  $\gamma_s = 1.15$ ). For  $\cot \theta = 1.0$  ( $\theta = 45^\circ$ ) the same reinforcement amount is needed in both directions, namely  $\rho_x = \rho_y = 1.13$  %. As actual reinforcement,  $\phi 14@100\text{mm}$  is placed in both sides and both directions (which corresponds to an actual reinforcement ratio of 1.23 %).

### 3.2.3 Design of the stringers

The horizontal stringers are integrated in the top and the bottom slabs and are in this context not critical. The design of the vertical stringers may be the most open topic as it allows for different interpretations. According to some recommendations, there will be the need to thicken the wall at the location of the stringer in order to limit the amount of force carried by the concrete of the stringer. For instance, according to Danish practice, if a minimum of one half of the load of the stringer shall be carried by the concrete, the wall thickness shall locally be increased to at least 370 mm in the stringer location ( $= (3700/2)/(20 \cdot 0.25)$ , adopted as 400 mm in the following). In addition to the concrete stringer, a compression reinforcement is also required to transfer the load through the slab to the stringer. According to recommendations where no limit is prescribed on the minimum force carried by the concrete (see for instance the Swiss code SIA 262:2013), the thickness of the stringer can be kept equal to 250 mm in the region of the stringer. The compression reinforcement necessary to transfer the load to the stringer is identical in both situations and can be calculated (neglecting confinement effects) as:

$$N_{d,s} = N_d - N_{Rd,c} = N_d - A_c \cdot \nu \cdot \frac{f_{ck}}{\gamma_c} \quad (9)$$

Where  $\nu$  refers to the strength reduction factor for the concrete in the stringer. According to Danish practice, this value can be adopted as  $\nu_m = 0.98 - f_{ck}/500$  [MPa] = 0.92. For other approaches, as MC2010, this value can be adopted equal to 1.0 ( $= \eta_{fc} \cdot \eta_\varepsilon$ ). In any case, this condition can be satisfied for instance by arrang-

ing a cage of compression reinforcement composed of 4 $\phi$ 40 TOP700 ( $f_{yk} = 700$  MPa,  $\gamma_s = 1.15$ ).

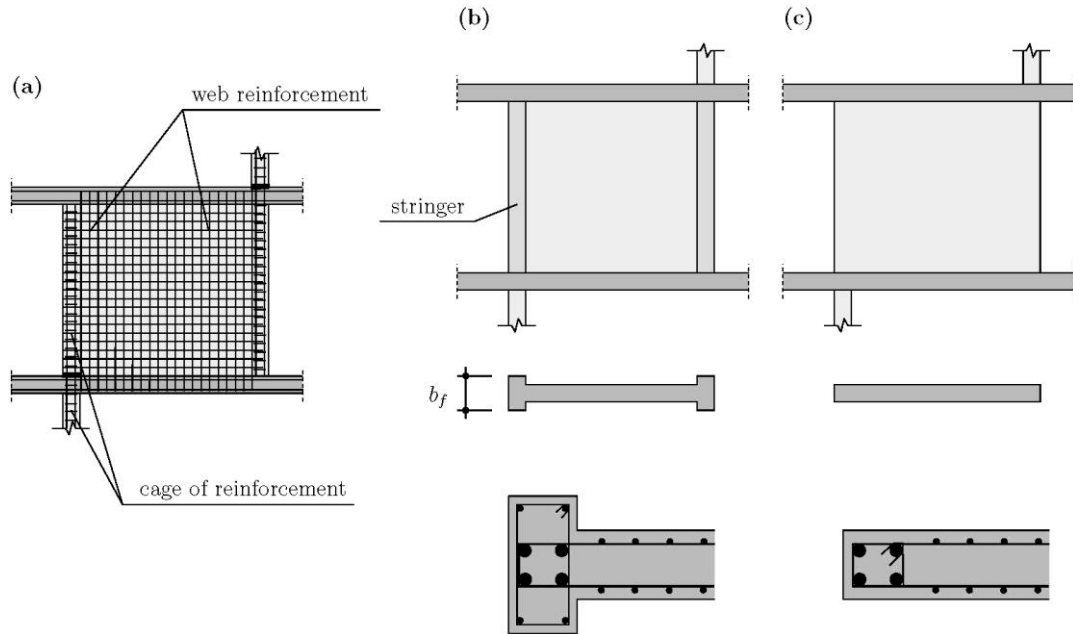


Figure 11: Investigated cases: (a) reinforcement layout; (b) wall with thick concrete stringers; and (c) wall with thin concrete stringers

### 3.2.4 Assessment of the strength of the member by using rigid-plastic stress fields

In the previous example, it shall be noted that the structure has a slightly larger web thickness than required (250 mm instead of 224 mm) and also slightly more reinforcement than needed. Consequently, the actual design strength, as determined by the Stringer Method, is larger than the design action (yielding of the mesh reinforcement governing):

$$N_{Rd} = \rho_y \cdot f_{yd} \cdot t \cdot z = 4017 \text{ kN} > N_{Ed} = 3700 \text{ kN} \quad (10)$$

The design results thus in a compliance factor (ratio of strength upon demand) equal to  $n = N_{Rd}/N_d = 1.08$ .

### 3.3 Discussion on the performance of the rigid-plastic solutions

The previous structural solutions with and without additional concrete in the location of the stringers will in reality lead to different performances when analysed with EPSF, allowing to discuss on their pertinence. To that purpose, three cases will be investigated by means of EPSF and compared in the following (same material and geometrical properties as the element designed in the previous section):

- A panel with the shear force introduced in a constant and distributed manner (in the closest possible manner to the Stringer Method, see Fig. 12a).
- A panel with horizontal flanges (corresponding to the slabs) and thick vertical stringers, see Fig. 12b. The effective width of the slabs (perpendicular to the wall plane) is considered equal to 2.0 m, assuming an angle of  $45^\circ$  for the forces spreading in the slab from the compression field of the web (compression field developing only at a certain region as it will later be discussed).
- A panel with horizontal flanges (as for the previous case) but without additional concrete at the vertical stringers, see Fig. 12c.

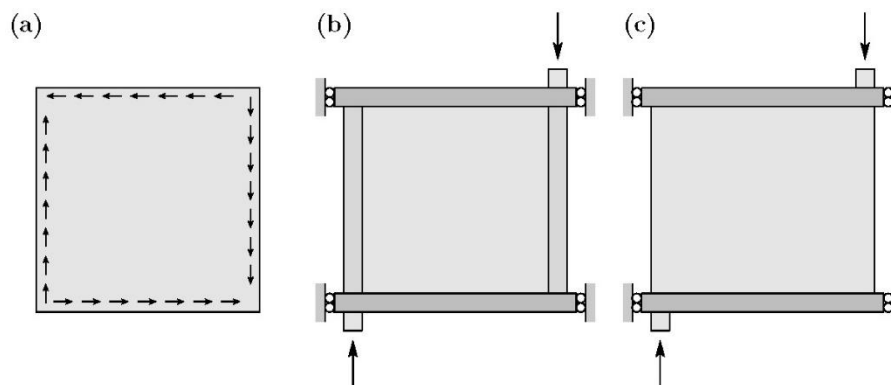


Figure 12: Boundary and load conditions modelling: (a) uniform shear force; (b) concentrated force introduction and thick concrete stringers; and (c) concentrated load introduction and thin concrete stringers

#### 3.3.1 Panel without stringers and subjected to uniform pure shear

The results for the first case are shown in Fig. 13, with the loads introduced in a uniform manner along the horizontal and vertical edges of the element (i.e. essentially a panel in pure shear). The failure load calculated by means of the EPSF results in a compliance factor  $n = N_{Rd}/N_d = 1.16$ . It can be noted that this compliance factor is higher than the one calculated according to the rigid-plastic analysis ( $n = 1.08$ ). This is justified by the actual value of the strength reduction factor accounting for the transverse strain state of concrete ( $\eta_\varepsilon$ ), which is equal to 0.60 according to the EPSF, but was assumed as 0.55 for the rigid-plastic design.

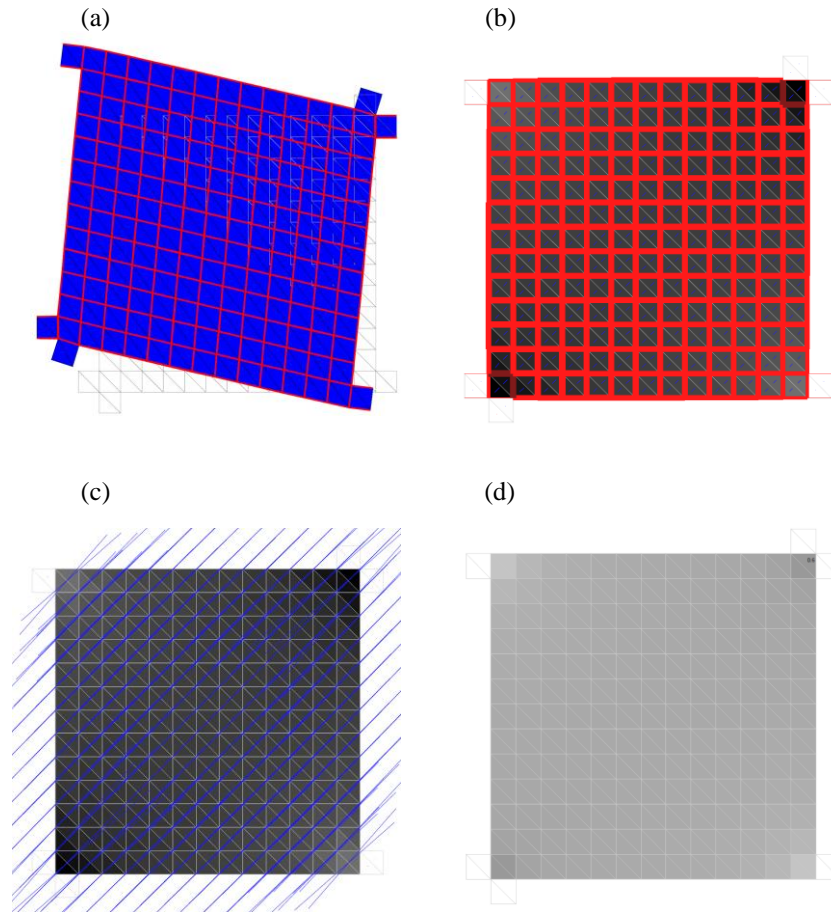


Figure 13: EPSF results for panel with uniform shear force: (a) deformed shape; (b) reinforcement utilization ratio (red for tension, blue for compression and brown for reinforcement yielding); (c) principal stress directions for concrete and calculated utilization ratio ( $\sigma_d / (f_{cp} \cdot \eta_\epsilon)$  where black means concrete crushing); and (d)  $\eta_\epsilon$  factor

### 3.3.2 Panel with thick stringers and with concentrated loads

The second case, corresponding to the panel with horizontal flanges and thick vertical concrete stringers, is presented in Fig. 14. The failure load yields in this case a compliance factor  $n = 1.15 = N_{Rd} / N_d$ . The failure mode is the same as for the first case (concrete crushing of the wall/panel) but the additional capacity of the thick stringers allows enhancing the resistance of the element. In fact, the stringers have the capacity to transfer a fraction of the total shear force by inclination of the compression chord developing inside (i.e. the stringers contribute also with a dowelling action).

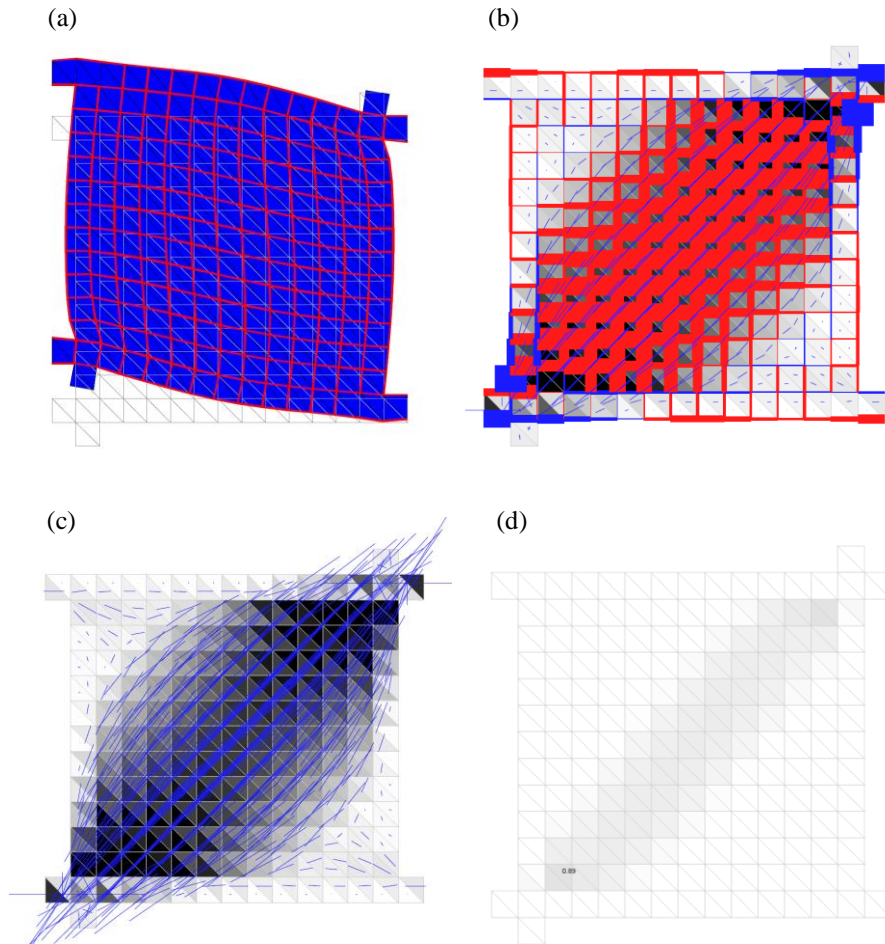


Figure 14: EPSF results for the wall with thick vertical concrete stringers: (a) deformed shape; (b) reinforcement utilization ratio (red for tension, blue for compression and brown for reinforcement yielding); (c) principal stress directions for concrete and calculated utilization ratio ( $\sigma_c/(f_{cp} \cdot \eta_\epsilon)$  where black means concrete crushing); and (d)  $\eta_\epsilon$  factor

In this case, however, the stress field differs significantly from the response of the panel in pure shear (Stringer Method and Fig. 13). Instead of having a uniform distribution of stresses, the compression field concentrates more in the inner part of the panel. The stresses are therefore locally higher than those of the rigid plastic solution and the effective strength of the concrete in this region is governing for the capacity of the structure. With this respect, when considering compatibility of the entire structure, the reduction of the concrete strength due to transverse cracking is less severe than in the case of a panel in pure shear, with a minimum value  $\eta_\epsilon = 0.89$  (see Fig. 14d.). The higher effectiveness factor obtained in this case is of course a result of the enhanced stiffness of the flanges and of the thick concrete stringers.

### 3.3.3 Panel with thin vertical concrete stringers and with concentrated loads

The last case corresponds to the member without a local thickening of the vertical concrete stringers, whose results are shown in Fig. 15. The failure load is again higher than the design load, with a compliance factor  $n = 1.03$ , but lower than the strength assessed with rigid-plastic stress fields ( $n = 1.08$ ).

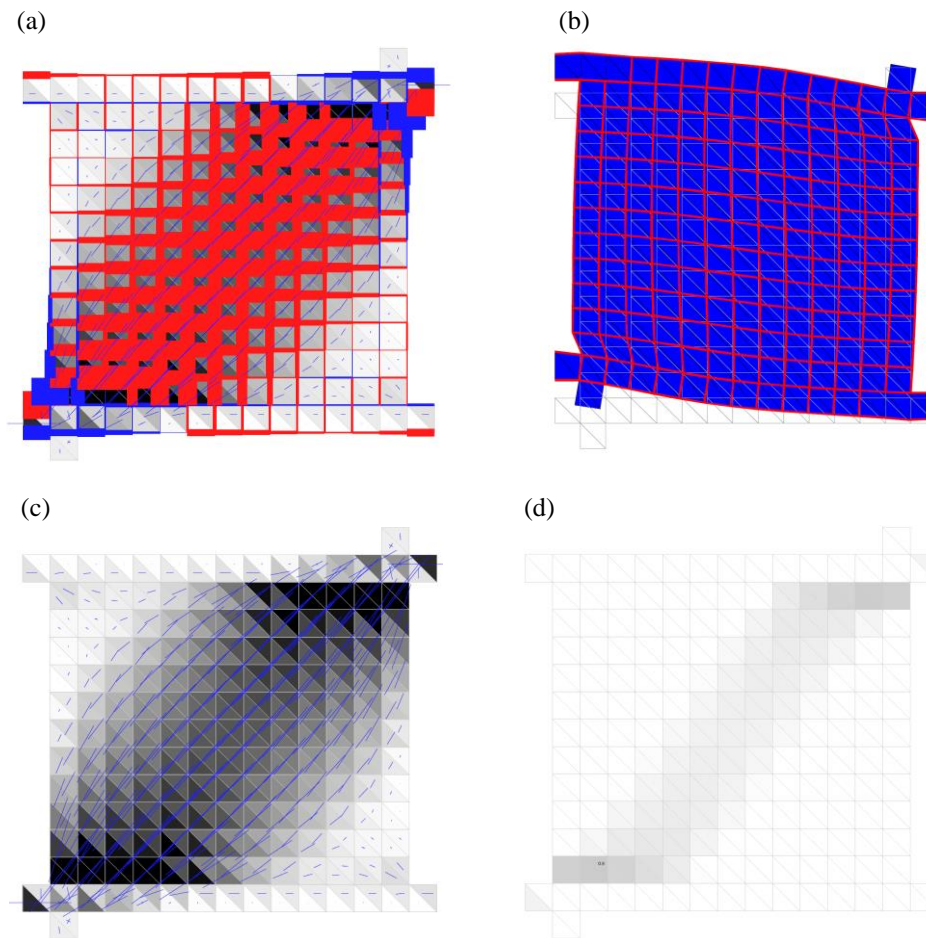


Figure 15: EPSF results for the wall with thin vertical concrete stringers: (a) deformed shape; (b) reinforcement utilization ratio (red for tension, blue for compression and brown for reinforcement yielding); (c) principal stress directions for concrete and calculated utilization ratio ( $\sigma_c/(f_{cp} \cdot \eta_\varepsilon)$  where black means concrete crushing); and (d)  $\eta_\varepsilon$  factor

The stress field is similar to the one of the member with thick vertical stringers, with a concentration of stresses in a compression field and with the capacity governed by the strength of concrete near the load introduction regions. In this case, as the stringers are less stiff (no local increase of concrete thickness), the value of coefficient  $\eta_\varepsilon$  reduces (minimum value of 0.8 at failure in the critical region) and leads, consistently, to a reduction of the failure load.

It can be noted that according to e.g. Swiss practice, reinforcing members as this one without thicker stringers is usually performed by arranging confinement stirrups near the introduction of concentrated loads (see Fig. 16). This is performed in order to enhance the ductility and resistance of concrete at the critical regions (due to the Kupfer's effect). This influence has yet not been considered in the previous analysis.

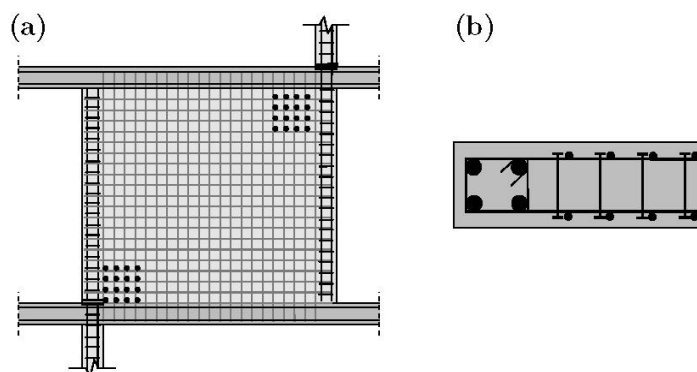


Figure 16: Enhancing the response of load-deviation walls without thicker concrete stringers: (a) location of additional confinement reinforcement near the load-introduction region; and (b) cross-section and detail

### 3.4 Behaviour of normally-reinforced elements

The previous case investigated an element where crushing of the concrete was governing in the EPSF analyses (i.e. the panel was over-reinforced). This condition makes the response of the element rather dependent on the value of the effectiveness factor for the concrete strength. In this section, the response of the member will be investigated also with reference to cases with lower reinforcement ratios (normally-reinforced elements). To that aim, both the vertical and horizontal reinforcements will be reduced down to the minimum values according to MC2010 (*fib*, 2013):

$$\rho_{w,\min} = 0.08 \frac{\sqrt{f_{ck}}}{f_{yk}} = 0.087\% \quad (11)$$

In this case, the resistance calculated according to the Stringer Method is linearly dependent on the amount of available mesh reinforcement (see Fig. 17). This solu-

tion, of course, is only a lower bound and does not reflect the potential load-carrying capacity for very low amounts of mesh reinforcement, where the load can be carried by a direct strut action, see Fig. 18a-b. This contribution can also be combined with inclined stress fields in the remaining triangular areas in order to obtain a larger capacity than the pure Stringer Method solution (Fig. 18c-d). Such solutions have been developed for shear walls by e.g. Liu (1997).

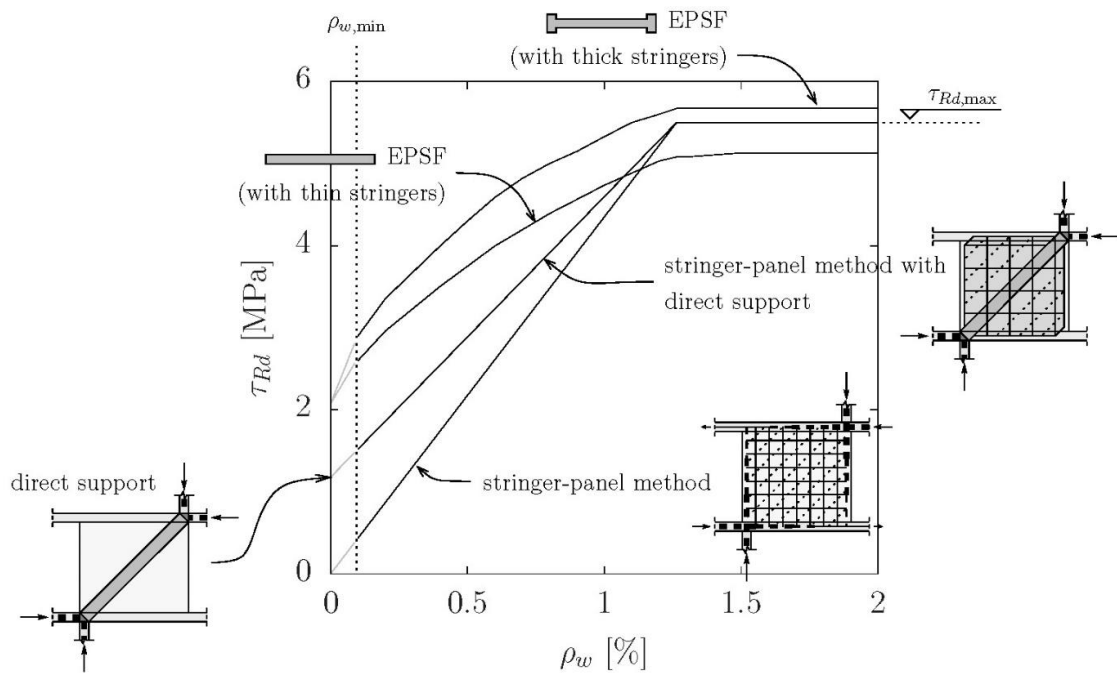


Figure 17: Design for the load-deviation wall according to different approaches: EPSF, Stringer-Method and Stringer-Method with consideration of direct support

For simplification purposes and on the safe side according to the theory of plasticity (convexity of yield surface), the response of the element considering the contribution of direct strut action can in this case be estimated as a linear interpolation between the direct strut action and the full web-crushing according to the Stringer Method (see Fig. 18). To that aim, a constant value for  $\nu$  equal to 0.55 is adopted (for both the smeared stress field and the direct strut) ensuring a consistent transition to the Stringer Method solution (it can be noted that the strength reduction factor could be considered equal to 1.0 for the case of direct strut action without any strained reinforcement or crack crossing it, but this value shall be reduced as the transverse reinforcement is strained and the model tends towards the Stringer Method solution).

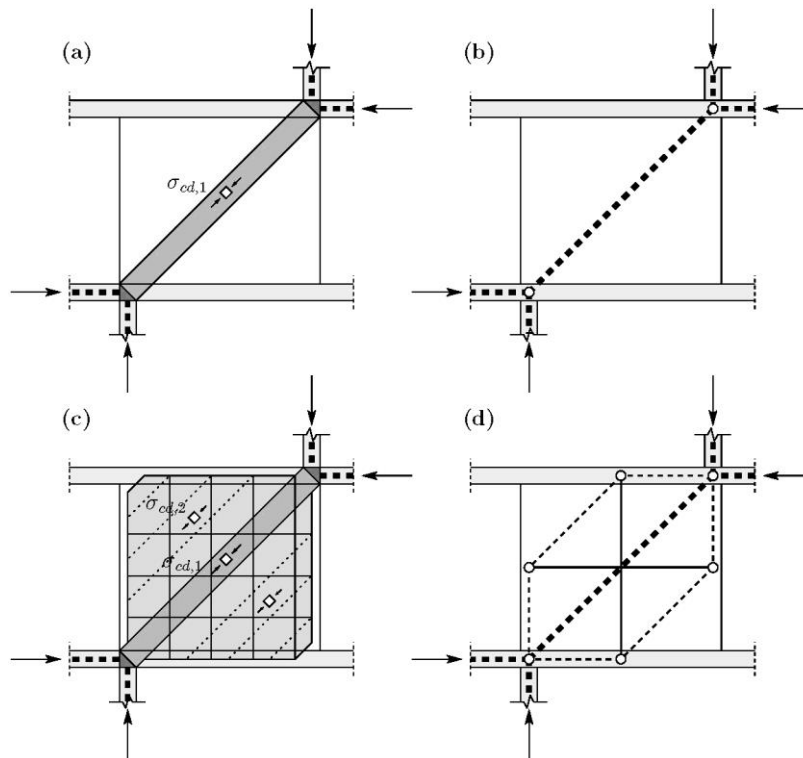


Figure 18: Direct support: (a) stress field model for direct support; (b) corresponding strut-and-tie model for (a); (c) stress field model of a direct support combined with a stringer-panel model; and (d) corresponding strut-and-tie model for (c)

The cases with and without local thickening of the vertical concrete stringers investigated by means of EPSF are also presented in Fig. 17 (where the width of the flanges is considered to be equal to the thickness of the web at pure direct support conditions). For increasing ratios of the mesh reinforcement, the strength is also observed to increase. Such increase is proportionally higher for low reinforcement ratios due to the progressive use of the horizontal stringers (slabs spreading the load) and to the more favourable values of the calculated strength reduction factors. For high reinforcement ratios, where the strength is controlled by crushing of the concrete, a complete smeared distribution of the compression field in the wall does not occur. The maximum possible capacity is, as previously commented, somewhat lower than the corresponding one of the stringer method (but higher than the design load) when no local thickening of the concrete stringers are considered and slightly higher when the presence of the thick stringers is considered.

#### 4. Conclusions

This paper presents the technique of the Elastic-Plastic Stress Fields (EPSF) and discusses its advantages and complementary use with respect to conventional Rigid-Plastic Stress Fields (RPSF). The main conclusions of this paper are listed below

- The classical limitations of RPSF (multiple solutions are possible, optimization and evaluation of efficiency factors) can be overcome by accounting for compatibility conditions when determining the stress field.
- EPSF are probably the simplest manner in which compatibility conditions can be accounted for in a stress field. Only the modulus of elasticity of the materials is to be considered in addition to the parameters defining the yield conditions of the materials. This ensures a maximum of consistency with RPSF.
- Since no tensile strength in concrete is considered in EPSF, the approach is very robust (provided that a minimum amount of reinforcement is available to control cracking) and the results are simple to interpret.
- The consideration of the strains in the member allow to locally evaluate the strain reduction factor associated to concrete cracking. This allows tailoring the stress fields to specific cases and removes the necessity to work with an average effectiveness factor for the entire member.
- At failure, EPSF provide not only a statically admissible and safe stress field but also a geometrically possible mechanism. Thus, EPSF can be used to obtain exact solutions according to the theory of plasticity. This fact is relevant for optimization of new structures, but it is also particularly relevant for the assessment of existing structures, as all potential load-carrying actions can be considered in a safe manner.
- The application of EPSF to practical cases (presented for a load-deviation wall in this paper) shows that the failure load can normally be increased compared to a prediction based on RPSF. It is also instrumental to perform the actual design of the structure (reinforcement, geometry of chords) according to the stress field considered.

## Notation

$A_c$	Cross-sectional area
$H_d$	Design value of the horizontal load
$N_d$	Design value of the axial load
$N_{d,s}$	Design value of the axial load carried by compression reinforcement
$N_{Rd}$	Design value of the strength of a member
$N_{Rd,c}$	Design value of the strength of concrete in compression
$V$	Shear force
$V_R$	Shear force at failure
$a$	Shear span
$f_c$	Uniaxial concrete strength measured in cylinder
$f_{ck}$	Characteristic value of the uniaxial concrete strength measured in cylinder
$f_{cp}$	Equivalent plastic strength
$f_y$	Yield strength of reinforcing steel
$f_{yd}$	Design value of the yield strength of reinforcing steel
$n$	Compliance factor
$t$	Thickness
$z$	Lever arm
$\delta$	Displacement
$\varepsilon_{1,2}$	Principal concrete strain
$\gamma_c$	Partial safety factor of concrete
$\gamma_s$	Partial safety factor of steel

$\eta_{fc}$	Brittleness factor reducing equivalent plastic concrete strength
$\eta_{\varepsilon}$	Strength reduction factor accounting for transverse strains in concrete
$\nu$	Effectiveness factor
$\nu_m$	Effectiveness factor for chords of beams in bending
$\theta$	Angle of compression field
$\rho_w$	Reinforcement ratio in the web ( $h, w$ corresponding to horizontal and vertical directions resp.)
$\rho$	Reinforcement ratio ( $x, y$ corresponding to the $x$ - and $y$ -directions resp.)
$\sigma_c$	Uniaxial concrete stress
$\sigma_{c1,2}$	Principal concrete stress
$\sigma_s$	Reinforcement stress
$\tau_{Ed}$	Design value of the acting shear stress
$\tau_R$	Shear strength
$\tau_{Rd}$	Design value of the shear strength

## Bibliography

- [1] Cardenas, A. E., Russell, H. G. and Corley, W. G. (1980), *Strength of Low-Rise Structural Walls*, American Concrete Institute, Special Publication 63, 1980, pp. 221-242
- [2] CEN European Committee for Standardization (2004), *Eurocode 2. Design of concrete structures – general rules and rules for buildings*, EN 1992-1-1, Brussels, Belgium; 2004. 225p.
- [3] Drucker, D. C. (1961), *On Structural Concrete and the Theorems of Limit Analysis*, International Association for Bridge and Structural Engineering, Zürich, Switzerland, 1961, 36 pp.
- [4] Fernández Ruiz, M., and Muttoni, A. (2007), “On Development of Suitable Stress Fields for Structural Concrete,” *ACI Structural Journal*, V. 104, No. 4, July-Aug. 2007, pp. 495-502.
- [5] *fib – The International Federation for Structural Concrete* (2013), *Model Code for Concrete Structures 2010*, Ernst & Sohn, Lausanne, Switzerland, 2013, 434 pp.
- [6] Fisker, J., Hagsten, L.G. (2016), ‘Mechanical Model for the Shear Capacity of R/C Beams without Stirrups: a Proposal Based on Limit Analysis’, *Engineering Structures*, Vol. 115, 2016, pp. 220-231.
- [7] Gvozdev, A. A. (1938) *Opredelenie velichiny razrushayuschei nagruzki dlya staticheskikh neopredelimykh sistem preterpevayuschikh plasticheskie deformatsii*, Moscow/Leningrad, Akademia Nauk SSSR, pp. 19-38, English translation: (1960), “The Determination of the Value of the Collapse Load for Statically Indeterminate Systems Undergoing Plastic Deformation,” *International Journal of Mechanical Sciences*, V. 1, No. 4, 1960, pp. 322-335
- [8] Herfelt, M.A (2017), *Numerical Limit Analysis of Precast Concrete Structures*, PhD thesis, Department of Civil Engineering, Technical University of Denmark, Lyngby, 2017, 250 pp.
- [9] Hoang L.C., Larsen B. and Jacobsen H.J. (2012), *Compressive strength of reinforced concrete disks with transverse tension*. *Bygningsstatistiske Meddelelser (Proceedings of the Danish Society for Structural Science and Engineering)*, Volume 83, No. 2-3, 23 – 61, 2012.

- [10] Jensen, U.G. (2011), *Limit Analysis of Reinforced Concrete Bridge Sub-structures*, PhD thesis, Institute of Technology and Innovation, University of Southern Denmark, Odense, 2011, 242 pp.
- [11] Larsen, K. P. (2010), *Numerical Limit Analysis of Reinforced Concrete Structures*. PhD thesis, Department of Civil Engineering, Technical University of Denmark, Lyngby, 2010. 140 pp.
- [12] Leonhardt, F., and Walther, R. (1966), *Wandartige Träger*, Deutscher Ausschuss für Stahlbeton, Berlin, Germany, 1966, 159 pp.
- [13] Liu, J. (1997), *Plastic theory applied to shear walls – Load-carrying capacity of shear walls*, PhD thesis, Dept. of Struct. Eng., Technical University of Denmark, Lyngby, 1997, 167 p.
- [14] Mörsch, E. (1908), *Der Eisenbetonbau, seine Theorie und Anwendung*, third edition, Verlag von Konrad Wittwer, Hamburg, Germany, 1908, 376 pp.
- [15] Mata Falcón, J. (2015). *Estudio del comportamiento en servicio y rotura de los apoyos a media madera*, PhD thesis, Universitat Politècnica de València, 2011, Spain, 747 pp.
- [16] Muttoni, A. (1989), “The Applicability of the Theory of Plasticity in the Design of Reinforced Concrete,” (“Die Anwendbarkeit der Plastizitätstheorie in der Bemessung von Stahlbeton”), Institut für Baustatik und Konstruktion, Bericht, No. 176, ETH Zürich, 1989, 159 pp. (in German)
- [17] Muttoni, A.; Schwartz, J.; and Thürlimann, B. (1997), *Design of Concrete Structures with Stress Fields*, Birkhäuser, Basel, Boston and Berlin, Switzerland, 1997, 145 pp.
- [18] Muttoni A., Fernández Ruiz M., Niketic F. (2015), *Design versus Assessment of Concrete Structures Using Stress Fields and Strut-and-Tie Models*, ACI Structural Journal, V. 112 No 5, Farmington Hills, USA, 2015, pp. 605-616.
- [19] Muttoni, A., Fernández Ruiz, M., Niketic, F., Backes, M.-R. (2016), *Assessment of Existing Structures based on Elastic-Plastic Stress Fields: Modelling of Critical Details and Investigation of the In-Plane Shear Transverse Bending Interaction*, Département fédéral des transports, des communications et de l'énergie, Office fédéral des routes, Rapport 680, Bern, Switzerland, 2016, 134 p.
- [20] Nielsen, M. P., and Hoang, L. C. (2011), *Limit Analysis and Concrete Plasticity*, third edition, CRC Press, Boca Raton, FL, 2011, 796 pp.

- [21] Prager, W. (1952), The general theory of limit design, Proc. 8<sup>th</sup> Int. Congr. Theor. Appl. Mech., Istanbul, 1952, vol. II, pp. 65-72
- [22] Ritter, W. (1899), “Die Bauweise Hennebique,” Schweizerische Bauzeitung, V. 33, No. 7, 1899, pp. 41-61.
- [23] Schlaich, J., and Weischede, D. (1982), “Ein praktisches Verfahren zum methodischen Bemessen und Konstruieren im Stahlbetonbau,” Bulletin d’Information No. 150, Comité Euro-International du Béton, Lausanne, Switzerland, 1982, 163 pp.
- [24] Schlaich, J.; Schäfer, K.; and Jennewein, M. (1987) “Toward a Consistent Design of Structural Concrete,” PCI Journal, V. 32, No. 3, 1987, pp. 74-150
- [25] Thürlimann, B.; Marti, P.; Pralong, J.; Ritz, P.; and Zimmerli, B. (1983), “Application of the Plasticity Theory to Reinforced Concrete,” (“Anwendung der Plastizitätstheorie auf Stahlbeton”), Institut für Baustatik und Konstruktion, ETH Zürich, 1983, 252 pp. (in German)
- [26] Vecchio, F. J., and Collins, M. P. (1986), “The Modified Compression-Field theory for Reinforced Concrete Elements Subjected to Shear,” ACI Journal Proceedings, V. 83, No. 2, Mar.-Apr. 1986, pp. 219-231.
- [27] Zhang, J.-P. (1997), Strength of cracked concrete, Part 3—Load carrying capacity of panels subjected to inplane stresses, Department of Structural Engineering and Materials, Technical University of Denmark, Report R, No. 18, 1997.



## DANSK SELSKAB FOR BYGNINGSSTATIK

Anmodning om optagelse i selskabet indsendes til et af bestyrelsens medlemmer:

Linh Cao Hoang (formand). Tlf. 45 25 17 06  
DTU, Institut for Byggeri og Anlæg, Brovej, 2800 Kgs. Lyngby

Niels Højgaard Pedersen (sekretær). Tlf. 72 44 75 34  
Vejdirektoratet, Guldalderen 12, 2640 Hedehusene

Lars Krog Christensen (kasserer). Tlf. 70 12 24 00  
MT Højgaard, Knud Højgaards Vej 9, 2860 Søborg

Uffe Graaskov Ravn. Tlf. 22 70 96 30  
COWI A/S, Parallelvej 2, 2800 Kgs. Lyngby

Srirengan Thangarajah. Tlf. 29 40 32 19  
Per Aarsleff A/S

Thomas Hansen. Tlf. 29 64 75 35  
ALECTIA A/S, Teknikerbyen 34, 2830 Virum

Carsten Munk Plum. Tlf. 45 66 10 11  
ES-Consult A/S, Sortemosevej 19, 3450 Allerød

Ronni Dam. Tlf. 51 61 61 19  
RAMBØLL, Hannemanns Allé 53, 2300 København S

Selskabets formål er at arbejde for den videnskabelige udvikling af bygningsmekanikken - både teori for og konstruktion af alle slags bærende konstruktioner - fremme interessen for faget, virke for et kollegialt forhold mellem dets udøvere og hævde dets betydning overfor og i samarbejde med andre grene af ingeniørvidevidenskaben. Formålet søges bl.a. realiseret gennem møder med foredrag og diskussioner samt gennem udgivelse af ”Bygningsstatiske Meddelelser”.

Som medlemmer kan optages personlige medlemmer, firmaer og institutioner, som er særligt interesserede i bygningsmekanik, eller hvis virksomhed falder indenfor bygnings-mekanikkens område.

Det årlige kontingent er for personlige medlemmer 300 kr., for firmaer samt institutioner 1.800 kr. Studerende ved Danmarks Tekniske Universitet og andre danske ingeniørskoler samt indtil 2-års kandidater kan optages som juniormedlemmer uden stemmeret for et årskontingent på 80 kr. Pensionerede medlemmer med mindst 10 års medlemsanciennitet kan opnå status som pensionistmedlem med stemmeret for et årskontingent på 100 kr.

Selskabets medlemmer modtager frit ”Bygningsstatiske Meddelelser”, der udsendes kvartalsvis. Endvidere publiceres ”Bygningsstatiske Meddelelser” på Selskabets hjemmeside [www.dsby.dk](http://www.dsby.dk). Manuskripter til optagelse i ”Bygningsstatiske Meddelelser” modtages af redaktøren.